

Real Time Implementation of A Fuzzy Logic Based Mppt Controller for Grid Connected Photovoltaic System

A. Menadi^{*‡}, S. Abdeddaim^{**}, A. Betka^{**}, M.T. Benchouia^{**}

* Electrical Engineering Department, laboratory LMSE, University of Biskra, Algeria

** Electrical Engineering Department, Laboratory LGEB, University of Biskra, Algeria
kimoumenadi@yahoo.fr, s_abdeddaim@yahoo.fr, betkaachour@gmail.com, benchouiat@yahoo.fr

‡Corresponding Author: A. Menadi, Universtity of Biskra, Algeria, Tel: +213 33 54 31 58,

Fax: +213 33 54 31 58, kimoumenadi@yahoo.fr

Received: 04.12.2014 Accepted: 13.02.2015

Abstract- The present work investigates a real time implementation of a photovoltaic grid connected chain, based on fuzzy logic MPPT controller (FLC). The implementation is realized on a dSPACE 1104 single board, controlling a boost chopper in the PV array side and a VSI inverter in the grid side. The FLC tracks permanently the maximum power point of the PV array without any prior information on the system model. The DC-link voltage controller is based on Lyapounov stability theory ensuring best performance for both transient and steady state, whereas, the hysteresis current controllers of the inverter allow a quasi-total transit of the maximum extracted PV power to the grid under unity power factor operation. The obtained results via Matlab-Simulink simulation are confirmed through experiment proving the effectiveness of the used control method.

Keywords—Photovoltaic, Grid connected, MPPT, FLC, Unity Power factor.

1. Introduction

Nowadays, renewable energy conversion has acquired a mature technology and provides a clean and inexhaustible source of energy for maintaining the continuously growing energy needs of humanity [1]. Among these renewable energy systems, solar power systems attract more attention because they provide excellent opportunity to supply far and isolate areas, as well as to share the power demand in the case of micro-grid with deep voltage. Tracking the Maximum Power Point (MPP) of a PV array is usually an essential part of a PV system, where many algorithms are applied to track the MPP. As exposed in [2], conventional methods such as Perturb & Observe (PO), do not have a good accuracy and response time, since oscillation occurs around the optimum in steady state. To overcome this drawback, several intelligent and complex control methods have been introduced recently. As depicted in [3], the authors implemented a robust control to track the MPP in real time using sliding mode control.

A new direction in development of MPP tracking is to use artificial intelligent control algorithms such as fuzzy logic, neural network [4], neuro-fuzzy MPPT strategy [5], and genetic algorithms [6]. The comparison between conventional and new intelligent algorithms proves a notable superiority of these artificial techniques, since the maximum power point is always tracked very fast regardless the sudden change of insolation without oscillations in permanent state, as mentioned in [7]. Furthermore, the transit of the extracted power to the grid is usually ensured through the regulation of the intermediate DC bus via a conventional PI controller; and where the selection of the controller's gains is usually subject to a continuous adjustment. There are several causes for this floating: external disturbance changing, saturation, noise, delays, and imperfections in signal acquisition [8, 9]. To overcome these drawbacks, the dc bus control design is inspired from the direct Lyapounov theory, ensuring an asymptotic stability of the system, and to obtain at the same time a proper matching of the predicted performances.

This paper investigates how an optimal operation of a small scale PV system connected to a micro grid can be achieved. The main tasks assigned to the proposed control strategy are:

1. A permanent tracking of the maximum power point of the PV array, by a proper adjusting of a boost chopper duty cycle, obtained via the fuzzy logic based MPPT control.
2. The conversion of the extracted PV energy to the utility, via the adjustment of the inverter's switching signals, under a unit power factor operation.

The paper is organized as follows. Section 2 presents the modeling of the different components of the system. Section 3 describes the proposed various control strategies. To test the effectiveness of these techniques, section 4 illustrates the obtained results for both simulation and experiment, while section 5 concludes the work.

2. System Description and Modeling

The power scheme of the studied system is shown in fig.1. The first stage of the conversion chain is composed of a PV array and a boost DC-DC converter serving as an impedance adapter and rises the relatively low optimum solar voltage to a suitable DC link voltage. The second stage is composed of a three phase voltage source inverter connected to the grid via an inductive filter.

Nomenclature

V_{PV} : photovoltaic array voltage (V)	V_{DC}, V_{DCref} : actual and reference DC link voltage (V)
I_{PV} : photovoltaic array current(A)	E, E_r : actual and reference insolation (W/m^2)
I_{sc} : photovoltaic short circuit (A) e_a :	I_a, I_b, I_c : grid currents (A)
I_o : inverse saturation current (A)	e_a, e_b, e_c : grid voltages (V)
V_{oc} : PV open circuit voltage (V)	$V_{a,b,c}$: inverter output voltages (V)
V_{th} : thermal voltage (V)	θ : grid estimated angle (rad)
R_s : array series resistance (Ω)	FLC : Fuzzy logic controller
α : chopper duty cycle	

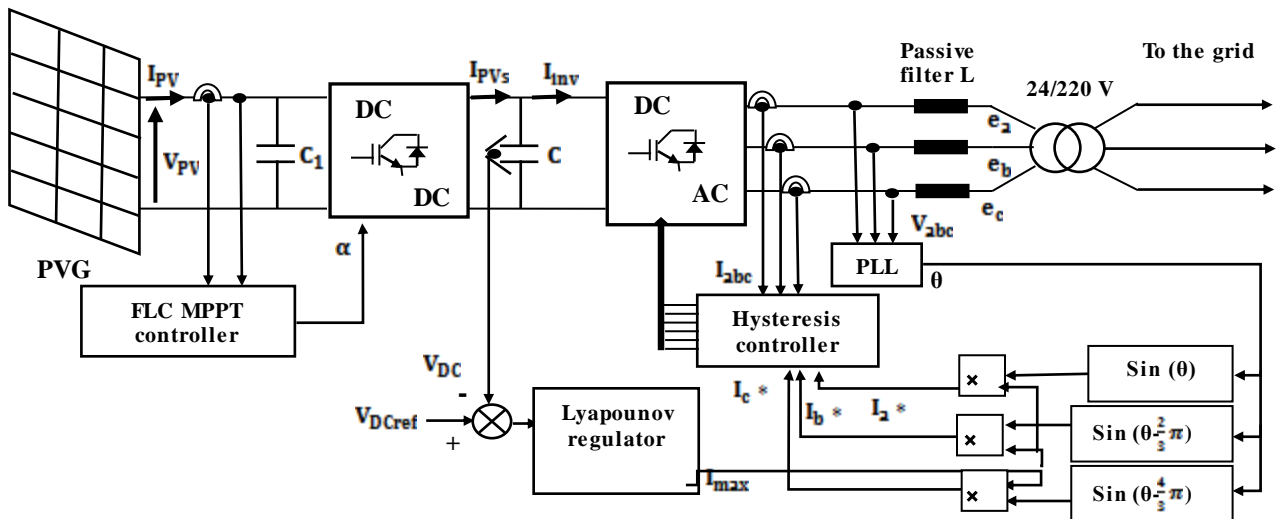


Fig.1. Synoptic scheme of the grid connected PV system.

$$I_{PV} = I_{sc} - I_o \left[\exp \left(\frac{V_{PV} + R_s I_{PV}}{V_{th}} \right) - 1 \right] \quad (1)$$

2.1. PV Array Modeling

Photovoltaic generators are neither voltage nor current sources, but can be approximated as current generators with dependent voltage sources, where the I-V characteristic can be expressed by an implicit equation[10]:

The I-V curve is nonlinear and crucially influenced by solar insolation and temperature variations. The adaption of eq. (1) to different levels of these inputs can be handled by the following equations[10]:

$$\Delta I = \beta \left(\frac{E}{E_r} \right) \Delta T + \left(\frac{E}{E_r} - 1 \right) I_{sc} \quad (2)$$

$$\Delta V = \gamma \Delta T - R_s \Delta I \quad (3)$$

$$V = V_r + \Delta V \quad (4)$$

$$I = I_r + \Delta I \quad (5)$$

2.2. DC-DC Converter Model

Referring to Fig.2, the state space averaging model is employed to describe the dynamic behavior of the DC-DC converter.

If the switch is in position S=0, the following expressions are synthesized:

$$L_1 \frac{di_{L1}}{dt} = V_{PV} - V_{DC} \quad (6)$$

$$C \frac{dV_{DC}}{dt} = i_{L1} - \frac{V_{DC}}{R_{ch}} \quad (7)$$

Whereas, in the position S=1, these differential equations are expressed as:

$$L_1 \frac{di_{L1}}{dt} = V_{PV} \quad (8)$$

$$C \frac{dV_{DC}}{dt} = i_C \quad (9)$$

Where R_{ch} denotes the system's equivalent load at the DC side.

The two equation sets (5,6), (6,7) are weighted by the duty ratio and added to get the average state space model of the converter:

$$\dot{x} = \alpha(A_1x + B_1V_{PV}) + (A_2x + B_2V_{PV})(1 - \alpha) \quad (10)$$

Where:
$$x = \begin{bmatrix} I_{L1} \\ V_{DC} \end{bmatrix}$$

Hence, the dynamic model of the converter can be rearranged as:

$$\dot{x} = \begin{bmatrix} 0 & -\frac{1-\alpha}{L_1} \\ -\frac{1-\alpha}{C} & -\frac{1}{R_{ch}C} \end{bmatrix} x + \begin{bmatrix} \frac{1}{L_1} \\ 0 \end{bmatrix} V_{PV} \quad (11)$$

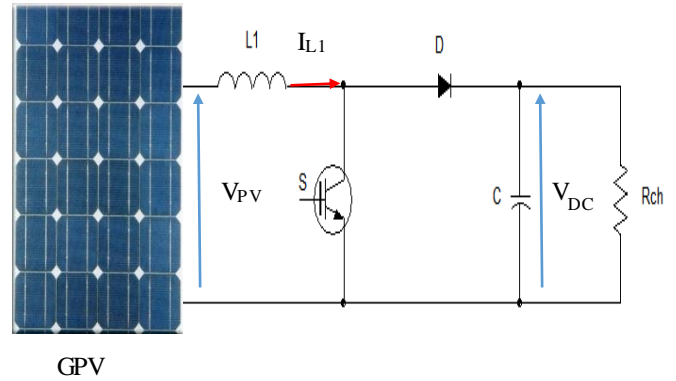


Fig.2. DC-DC boost converter scheme

2.3. Voltage Source Inverter Model

The used DC-AC converter is a two level voltage source inverter with three independent arms. Each one includes two IGBTs switches, complementary switched, and controlled by the Pulse Width Modulation strategy. The inverter acts as a power controller between the DC-link and the grid.

The inverter's output voltages (V_a , V_b , V_c) as well as the inverter current in the DC side I_{inv} are related to the switching states K_1 , K_2 and K_3 as[11]:

$$\begin{bmatrix} V_a \\ V_b \\ V_c \end{bmatrix} = \frac{V_{DC}}{3} \begin{bmatrix} 2 & -1 & -1 \\ -1 & 2 & -1 \\ -1 & -1 & 2 \end{bmatrix} \begin{bmatrix} K_1 \\ K_2 \\ K_3 \end{bmatrix} \quad (12)$$

$$I_{inv} = K_1 i_a + K_2 i_b + K_3 i_c \quad (13)$$

2.4. Grid model:

The dynamic model of the utility in the inverter side is obtained via a simple addition of both no-load voltages e_a , e_b , e_c and voltages across the inductive filters:

$$\begin{cases} V_a = I_a * R + L * \frac{di_a}{dt} + e_a \\ V_b = I_b * R + L * \frac{di_b}{dt} + e_b \\ V_c = I_c * R + L * \frac{di_c}{dt} + e_c \end{cases} \quad (14)$$

3. Control Approaches

3.1. PV Side Control

Due to non-linear I-V characteristics of the photovoltaic array, a maximum power point tracking algorithm is adopted to extract the optimum PV power regardless solar insolation, temperature and load variations. Among the two last decades, several algorithms have been developed and addressed in many literatures in order to achieve maximum power point tracking. These techniques vary between them in many aspects including simplicity, oscillations around MPP,

convergence speed, hardware implementation, sensors required, cost, range of effectiveness and need for parameterization[12].

Recently, Microcontrollers have made using fuzzy logic control more attraction for MPPT. The FLC have the advantages of working with imprecise inputs, not needing for an accurate mathematical model, and handling non linearity [13].

3.1.1. Fuzzy logic MPPT controller:

For the MPP fuzzy logic tracking method, the regulator synthesis passes through the set of four conventional steps: fuzzification, rule bases, fuzzy inference and defuzzification, as shown in Fig.3.

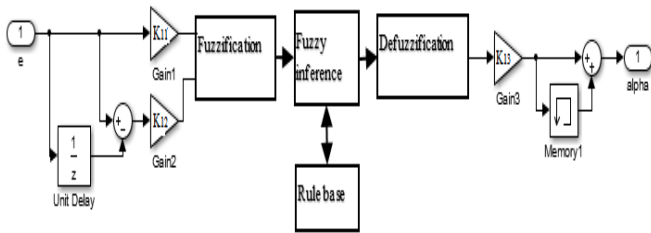


Fig.3. Fuzzy Logic MPPT controller.

The search pattern is conducted through the adjustment of the boost chopper duty cycle, provided by the fuzzy logic controller, according to the variation of the two following inputs e and Δe :

$$e = \frac{\Delta V_{PV}}{\Delta I_{PV}} * I_{PV} + V_{PV} \tag{15}$$

$$\Delta e = e(k) - e(k-1) \tag{16}$$

Where:

ΔV_{PV} and ΔI_{PV} are the PV array voltage and current changes, sensed at two sampling time k and $(k-1)$.

The error equation in (15) describes the incremental conductance condition, which converges to zero once the optimum point is tracked.

To avoid hard calculation, triangle membership functions were chosen for both input and output as depicted in fig.4.

To get an accurate tracking of the optimum MPP point in the case of large insolation variation, forty nine fuzzy rules, with the following linguistic variables have been chosen.

NB: Negative Big, NM: Negative Medium, NS: Negative Small, ZE: Zero, PS: Positive Small, PM: Positive Medium, PB: Positive Big.

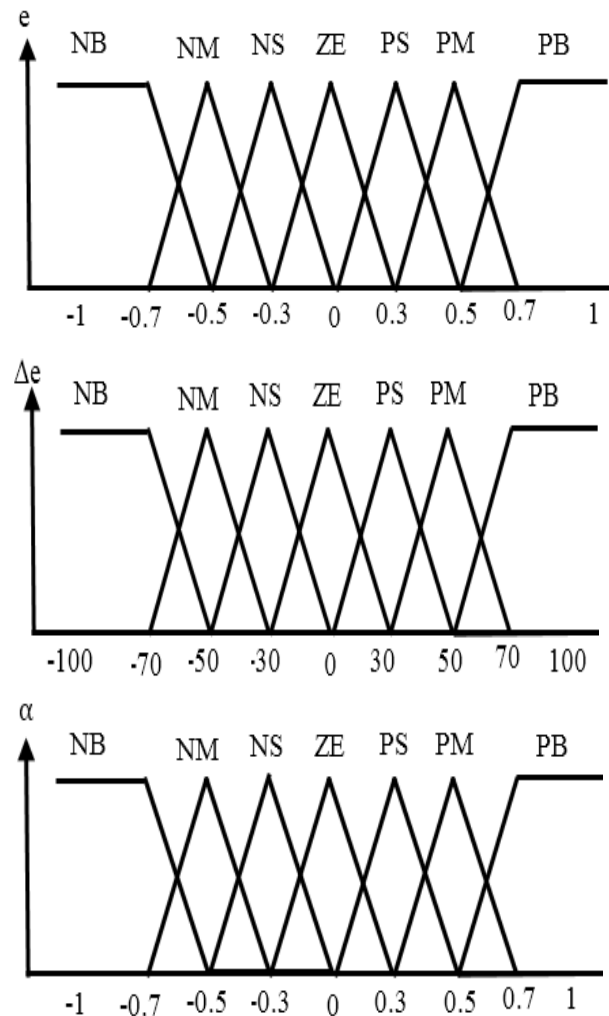


Fig.4. Membership functions of the input and the output

The PV power difference (ΔP) will be increased or decreased in the positive or in the negative direction with a small or a large value until it approximates the MPP and the error almost equals zero.

E \ Δe	NB	NM	NS	ZE	PS	PM	PB
NB	NB	NB	NB	NB	NM	NS	ZE
NM	NB	NB	NB	NM	NS	ZE	PS
NS	NB	NB	NM	NS	ZE	PS	PM
ZE	NB	NM	NS	ZE	PS	PM	PB
PS	NM	NS	ZE	PS	PM	PB	PB
PM	NS	ZE	PS	PM	PB	PB	PB
PB	ZE	PS	PM	PB	PB	PB	PB

Table .1. Rule base for the MPPT algorithm

The fuzzy inference step is carried out by the Mamdani's method (Table.1.), whereas the defuzzification uses the

center of gravity method to compute the increment duty cycle $\Delta\alpha$:

$$\Delta\alpha = \frac{\sum_{i=1}^p (d\alpha_i \cdot u_i)}{\sum_{i=1}^p u_i} \quad (17)$$

The three normalization gains K_{11} , K_{12} allow to convert the real input values into fuzzy quantities and K_{13} provides the real value of the output fuzzy amount.

3.2. Grid Side Control

To permit a total flow of the extracted power in the grid, the voltage source inverter control is performed in a cascade manner. The robust controller of the DC link voltage ensures through the grid current control a unity power factor functioning.

3.2.1. DC link voltage controller:

To maintain constant the DC link voltage at a reference value regardless the system disturbances, a robust controller based on the Lyapunov theory is chosen, where a global asymptotic stability of the system is ensured.

The dynamic equation of the DC link voltage is given by [14]:

$$C \frac{dV_{DC}}{dt} = I_{PVs} - I_{inv} \quad (18)$$

The regulation of the DC link voltage is carried out by the inverter current I_{inv} in the DC side, whereas I_{PVs} is considered as a disturbance.

One can define a quadratic positive function related to the tracking error:

$$V = \frac{1}{2} * e^2 \quad (19)$$

Where the DC link voltage error is defined as:

$$e = V_{DC} - V_{DCref} \quad (20)$$

Hence, the gradient of the cost function V is derived as:

$$\dot{V} = \dot{e}e \quad (21)$$

To ensure an asymptotic stability of the system, eq. (21) must be semi negative defined. Let's choose the desired gradient function as follows:

$$\dot{V} = -Ke^2 \quad (22)$$

By a proper tuning of the constant K , the system dynamics are improved, and the DC link voltage tracks its reference in a finite time.

By equaling eq (21) and eq (22), the closed loop error dynamic is derived as a stable first order equation:

$$\dot{e} = -Ke \quad (23)$$

Consequently, the inverter current on the DC side is deduced as:

$$I_{inv} = I_{PVs} + K * C * e \quad (24)$$

3.2.2. Inverter current control:

The VSI control is performed in current mode via simple hysteresis controllers, where the measured grid currents I_a , I_b , I_c match their references according to a preset hysteresis band Δi . Firstly, the reference current peak value I_{max} and the grid angle θ are deduced before the switching of the inverter's three legs starts.

Assuming an operation with a unit power factor in the grid side, the peak value of the AC current I_{max} is related to I_{inv} through the following linear equation:

$$I_{inv} = K_c * I_{max} \quad (25)$$

Where the coefficient K_c is computed on the basis of lossless inverter and a quite regulation of the DC link voltage at its reference value V_{DCref} [15]:

$$K_c = \frac{\sqrt{3}}{\sqrt{2}} \frac{V}{V_{DCref}} \quad (26)$$

To achieve a synchronization with the grid voltage, a phased locked loop (PLL) is used. It provides in real time the grid phase θ and frequency in the basis of grid voltage orientation on the q-axis ($V_{rd} = 0$ and $V_{rq} = -\sqrt{3}V_{rms}$).

The PI regulator should be designed to respond with minimum overshoot to grid frequency and voltage variations.

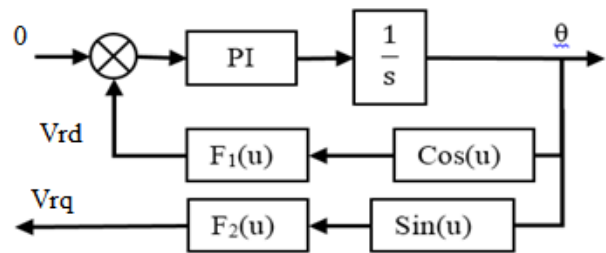


Fig.5. Phase locked loop (PLL) scheme.

The amplitude of the reference current I_{max} takes care of the active power demand on the grid side and the system's losses. Thus, the switching signals of the inverter are obtained by comparing the measured grid currents (I_a, I_b, I_c) with their reference quantities (I_a^*, I_b^*, I_c^*) through Schmidt flip flops.

4. Obtained Results

4.1. Simulation Results

To test the effectiveness of the proposed control strategies, simulation tests are firstly conducted, where the solar insolation level is varied with steps of 200W/m², as shown on fig.6.

On fig.7 and fig.8 are depicted the PV array current and power respectively, plotted together with the off-line optimal quantities. One can notice that:

- The PV array current and power track the optimal off-line values (I_{op-ref} , P_{op-ref}) despite the insolation level variations, which consequently proves the robustness of the introduced FLC based MPPT controller.
- The current and power amounts increase monotonically with the solar insolation, since the PV voltage is less affected by the insolation variation than the current.

Fig.9 shows the DC link voltage regulation, where the reference value changes abruptly from 150V to 200V at 2s. One remarks that the measured voltage tracks its reference with good tracking dynamics without overshoot. Besides, the following performance index I_1 is quantified. The calculated surface I_1 permits to check the speed of the transient step.

$$I_1 = \int |e(t)| dt \quad (27)$$

The small obtained value ($I_1 = 1.45$) proves consequently that the Lyapunov controller is fast and efficient.

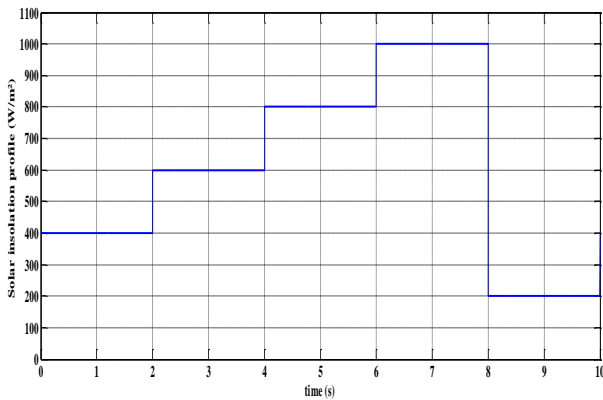


Fig.6. Solar insolation profile.

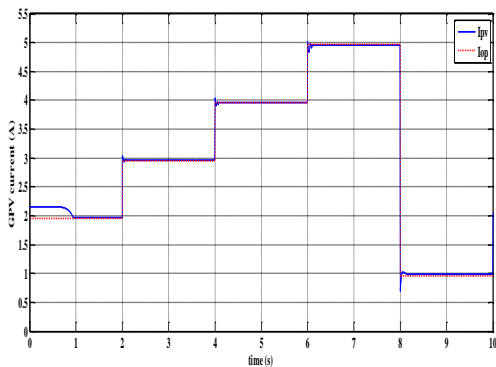


Fig.7. PV array current.

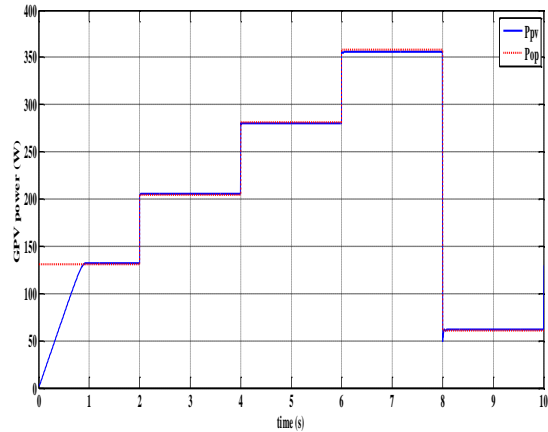


Fig.8. PV array power.

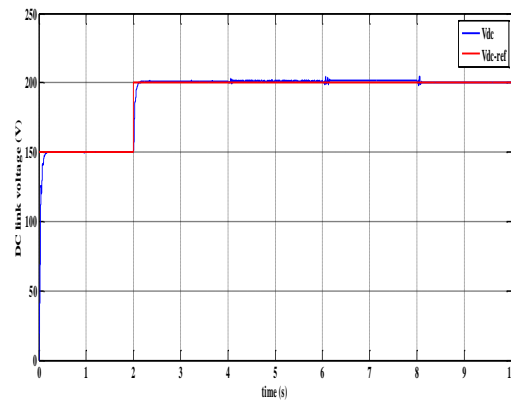


Fig.9. DC link voltage.

Finally, on fig.10 are illustrated a sample of the phase voltage, the reference and the measured current curves on the grid side. One remarks that the hysteresis controller proves a notable efficiency since the phase current tracks closely its reference. Furthermore, the phase voltage and current are kept in phase, leading to a unit power factor functioning.

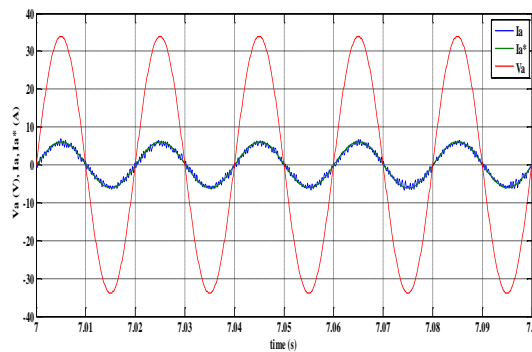


Fig.10. phase voltage, measured and reference current curves

4.2. Experimental Validation

To validate practically the obtained simulation results, a test rig was built in LGEB laboratory, where the PV array consists of two PV modules of 175 Wper each, connected in parallel and fixed on the roof. The boost chopper is composed of one IGBT module, switched at 15 kHz, and the voltage source inverter is a didactic Semikron converter, built around three IGBT arms with a common capacitive DC link. The inverter is connected to the utility via a passive filter and a step up transformer of 24/220 V.

The control algorithm is implemented with a dSPACE 1104 card from Texas Instrument with a TMS320F240 DSP (20 MHz) and a microprocessor Power PC 603e (250 MHz) (lower part).

The connections between the dSPACE card and the power converter are carried out by an interface card, which adapts the control signal levels to the IGBT’s driver voltage. The different currents and voltages are ensured by the (LA25NP) and (LV25P) sensors, as depicted on fig.11.

The different data of the system are given in appendix.

The experiment was conducted in a clear day, the 25th of April 2014, where the solar insolation varies very slowly.

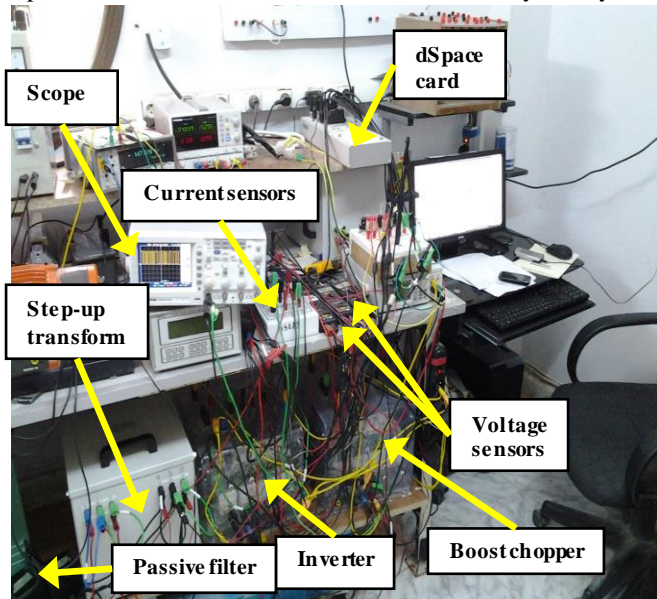


Fig.11. Experimental test bench

Figures.(12) and (13) depict the performances of the proposed MPPT based fuzzy controller, showing the PV generator voltage and current curves. Firstly, the PV array was kept disconnected from the system and the VS inverter current control is allowed. The PV generator current remains equal to zero until point A. At this moment, the fuzzy MPPT algorithm is compiled. As can be seen, the PV operating point (current, voltage) moves towards the optimum MPP zone (point B) aperiodically with a small oscillation, since

the incremental conductance condition $(\frac{dI_{pv}}{dV_{pv}} V_{pv} + I_{pv} = 0)$, shown in fig.13 remains full filled.

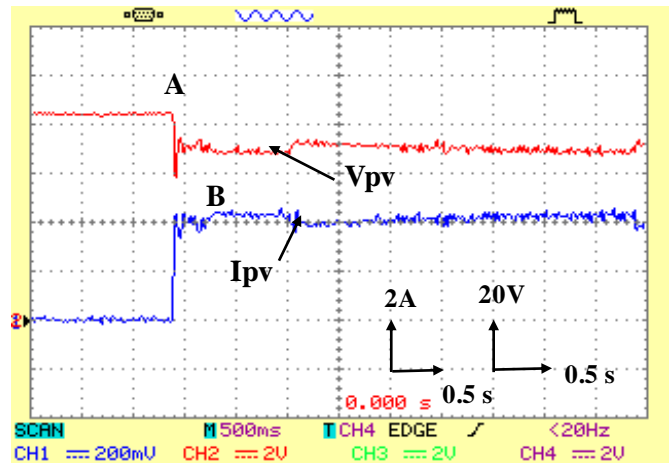


Fig.12. Experimental PV voltage and current curves

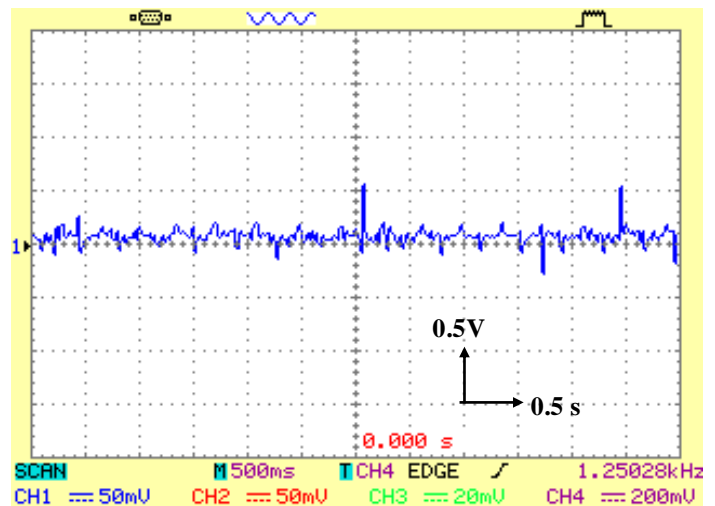
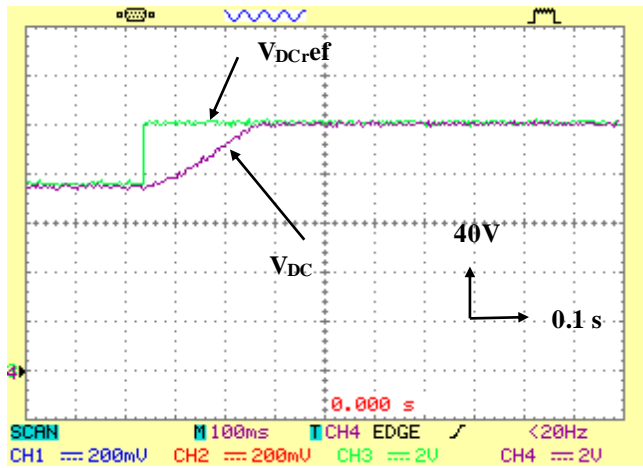


Fig.13. Accuracy of the fuzzy Logic MPPT controller

Fig.14 shows the shape of the DC- link voltage, where a sudden step change of the reference value was applied at t= 0.23s (from 150v to 200v). As can be seen, the actual voltage tracks its reference quietly without overshoot. In addition, to prove the efficiency of the chosen controller in a comparative way, fig. 14.b plots the dc bus voltage curve under a PI based control. One can notice that the system dynamics are clearly improved in case (a), where the Lyapounov controller arrives fast to reject the PV current effect and the settling time approaches 1/3 of case (b).



a. Lyapunov controller.

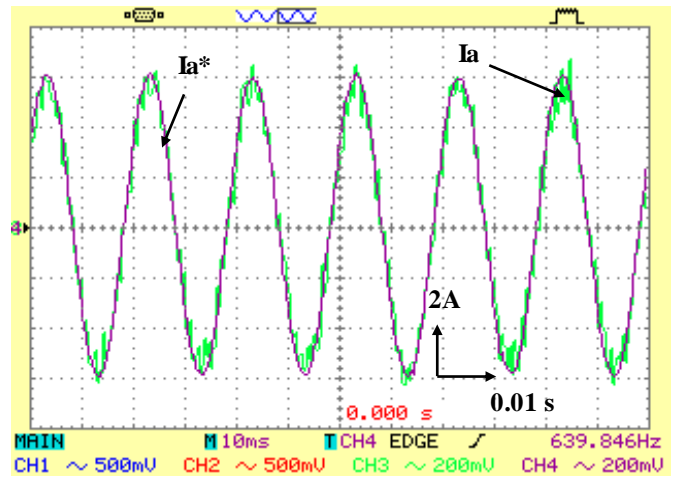
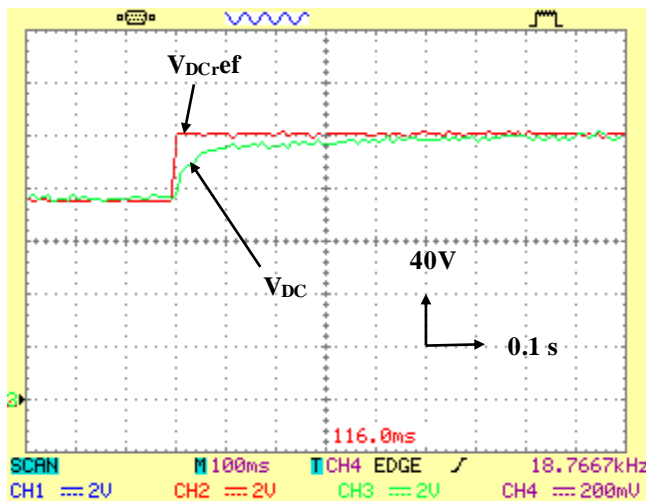


Fig.15. Grid current with its reference



b. PI controller.

Fig.14. The DC-link voltage curve.

Figure.15. shows the phase current and its reference, whereas fig.16 illustrates both the grid voltage and current curves.

From these figures, the two following remarks are extracted:

- The hysteresis current controller proves its robustness, since the phase current tracks its reference perfectly.
- The system operates with a unit power factor since the grid voltage and current are in phase, which permits consequently a total flow of the extracted PV power to the grid. Such performances can be used to support the grid, operating with deep voltage.

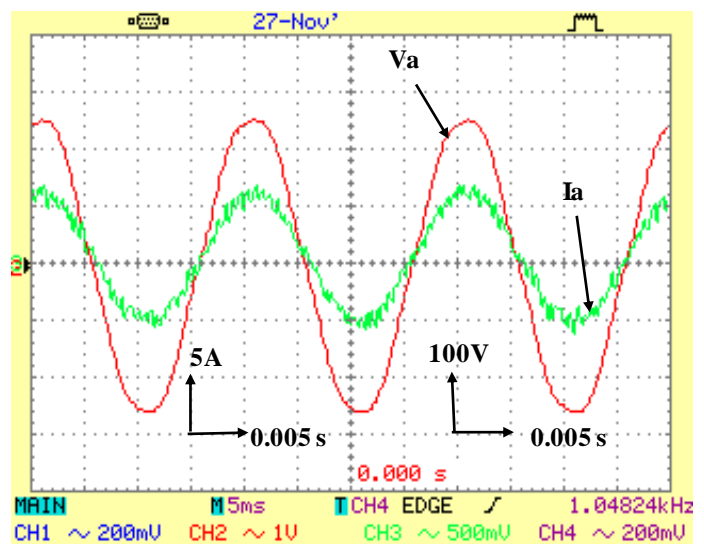


Fig.16: Grid voltage and current curves

5. Conclusion

In this work, a real time implementation of a small scale grid connected photovoltaic system was presented. The various control techniques have been tested through simulation and validated with experiment, providing similar performances. The fuzzy logic based MPPT controller provides a notable efficiency, since it permits to track the optimum power quickly despite the atmosphere condition changing. Besides, the regulation of the DC link voltage based on Lyapunov theory, and the current control of the VS inverter has permitted an operation of the system under a unit power factor.

Appendix:

- 1) Data of the PV array at STC conditions (Sharp):

$P_{PV} = 350 \text{ W}$, $I_{sc} = 5.4 \text{ A}$, $V_{oc} = 88.8 \text{ V}$, $I_{op} = 4.95 \text{ A}$,
 $V_{op} = 70.8 \text{ V}$.

2) Passive filters:

$C1 = 330 \mu\text{F}$, $C = 1100\mu\text{F}$, $L = 10 \text{ mH}$

3) Controllers parameters:

➤ FLC gains: $K11=0.006$; $K12=0.01$; $K13=50$

➤ Lyapounov gain: $K=40$

➤ Hysterisis band: $\Delta i = 0.01$

➤ PLL function:

$F_1(u) = V_{\alpha} \cos(\theta) + V_{\beta} \sin(\theta)$

$F_2(u) = V_{\beta} \cos(\theta) - V_{\alpha} \sin(\theta)$

References

- [1] I. Purnama, Y.-K. Lo, and H.-J. Chiu, "A fuzzy control maximum power point tracking photovoltaic system," in *fuzzy systems (FUZZ)*, 2011 IEEE international conference on, 2011, pp. 2432-2439.
- [2] K. Ishaque, Z. Salam, and G. Lauss, "The performance of perturb and observe and incremental conductance maximum power point tracking method under dynamic weather conditions," *Applied Energy*, vol. 119, pp. 228-236, 2014.
- [3] C.-C. Chu and C.-L. Chen, "Robust maximum power point tracking method for photovoltaic cells: A sliding mode control approach," *Solar Energy*, vol. 83, pp. 1370-1378, 2009.
- [4] Y.-H. Liu, C.-L. Liu, J.-W. Huang, and J.-H. Chen, "Neural-network-based maximum power point tracking methods for photovoltaic systems operating under fast changing environments," *Solar Energy*, vol. 89, pp. 42-53, 2013.
- [5] A. Chaouachi, R. M. Kamel, and K. Nagasaka, "A novel multi-model neuro-fuzzy-based MPPT for three-phase grid-connected photovoltaic system," *Solar Energy*, vol. 84, pp. 2219-2229, 2010.
- [6] Y. Shaiek, M. Ben Smida, A. Sakly, and M. F. Mimouni, "Comparison between conventional methods and GA approach for maximum power point tracking of shaded solar PV generators," *Solar Energy*, vol. 90, pp. 107-122, 2013.
- [7] M. Mohd Zainuri, M. Radzi, A. C. Soh, and N. A. Rahim, "Adaptive P&O-fuzzy control MPPT for PV boost dc-dc converter," in *Power and Energy (PECon)*, 2012 IEEE International Conference on, pp. 524-529, 2012.
- [8] P. Li, C. Liu, W. Li, Z. Yin, J. Chen, and K. Liu, "The research on photovoltaic power flexible grid-connected in microgrid based on H_{∞} control," in *Power System Technology (POWERCON)*, 2012 IEEE International Conference on, pp. 1-6, 2012.
- [9] X. Chen, Q. Fu, S. Yu, and L. Zhou, "Unified control of photovoltaic grid-connection and power quality managements," in *Power Electronics and Intelligent Transportation System, 2008. PEITS'08. Workshop on*, pp. 360-365, 2008.
- [10] A. Betka and A. Attali, "Optimization of a photovoltaic pumping system based on the optimal control theory," *Solar Energy*, vol. 84, pp. 1273-1283, 2010.
- [11] R. Marouani and A. Mami, "Voltage oriented control applied to a grid connected photovoltaic system with maximum power point tracking technique," *American Journal of Applied Sciences*, vol. 7, p. 1168, 2010.
- [12] K. Barra and D. Rahem, "Predictive direct power control for photovoltaic grid connected system: An approach based on multilevel converters," *Energy Conversion and Management*, vol. 78, pp. 825-834, 2014.
- [13] A. A. Ovalle, H. Chamorro, and G. Ramos, "Improvements to MPPT for PV generation based on Mamdani and Takagi-Sugeno fuzzy techniques," in *Transmission and Distribution: Latin America Conference and Exposition (T&D-LA)*, 2012 Sixth IEEE/PES, 2012, pp. 1-6.
- [14] N. Hamrouni, M. Jraidi, and A. Cherif, "New control strategy for 2-stage grid-connected photovoltaic power system," *Renewable Energy*, vol. 33, pp. 2212-2221, 2008.
- [15] M. Matsui, T. Kitano, and D. Xu, "A simple maximum photovoltaic power tracking technique utilizing system inherent limit cycle phenomena," in *Industry Applications Conference, 2003. 38th IAS Annual Meeting. Conference Record of the*, pp. 2041-2047, 2003.